Oxygen Permeation Resistance of Polyethylene, Polyethylene/Ethylene Vinyl Alcohol Copolymer, Polyethylene/Modified Ethylene Vinyl Alcohol Copolymer, and Polyethylene/Modified Polyamide–Ethylene Vinyl Alcohol Copolymer Bottles

Jen-Taut Yeh,[1,2] Shyh-Shiuan Huang,[2] Wei-Hua Yao,[2] Ing-Jing Wang,[2] Cheng-Chi Chen[3]

[1]Faculty of Chemistry and Material Science, Hubei University, Wuhan, China
[2]Graduate School of Fiber and Polymer Engineering, National Taiwan University of Science and Technology, Taipei, Taiwan
[3]Department of Chemical Engineering, Nanya Institute of Technology, Jhongli, Taoyuan, Taiwan

ABSTRACT: The oxygen permeation resistance of polyethylene (PE), polyethylene/ethylene vinyl alcohol copolymer (PE/EVOH), polyethylene/modified ethylene vinyl alcohol copolymer (PE/MEVOH), and polyethylene/modified polyamide–ethylene vinyl alcohol copolymer (PE/MPAEVOH) bottles was investigated. The oxygen permeation resistance improved significantly after the blending of ethylene vinyl alcohol copolymer (EVOH) barrier resins in PE matrices during blow molding; less demarcated EVOH laminas were found on the fracture surfaces of the PE/EVOH bottles. Surprisingly, the oxygen permeation resistance of the PE/MEVOH bottles decreased significantly, although more clearly defined modified ethylene vinyl alcohol copolymer (MEVOH) laminas were found for the PE/MEVOH bottles as the compatibilizer precursor contents present in the MEVOH resins increased. In contrast, after the blending of modified polyamide (MPA) in EVOH resins, more demarcated modified polyamide–ethylene vinyl alcohol copolymer (MPAEVOH) laminar structures were observed in the PE/MPAEVOH bottles as the MPA contents present in the MPAEVOH resins increased. In fact, with proper MPAEVOH compositions, the oxygen permeation resistance of the PE/MPAEVOH bottles was even better than that of the PE/EVOH bottles. These interesting oxygen barrier and morphological properties of the PE, PE/EVOH, PE/MEVOH, and PE/MPAEVOH bottles were investigated in terms of the free volumes, barrier properties, and molecular interactions in the amorphous-phase structures of the barrier resins present in their corresponding bottles. © 2004 Wiley Periodicals, Inc. J Appl Polym Sci 92: 2528–2537, 2004

Key words: barrier; blending; oxygen permeation

INTRODUCTION

Organic liquids such as hydrocarbons and chlorinated solvents can easily permeate polyethylene (PE). The ethylene vinyl alcohol copolymer (EVOH) and polyamide (PA), known for their excellent transparency, oil resistance, and outstanding barrier properties against nonpolar gas and solvent permeation,[1–3] are recognized as oxygen-barrier materials in packaging applications for food and other products that require protection from oxygen.[4–6] However, because of their expensiveness and brittle properties, EVOH resins are often coextruded or blended with other polymers.[7,8] For example, blends of EVOH with lower cost high-density polyethylene (HDPE) with high impact resistance would be desirable. Most commercially available EVOH materials contain 55–75 mol % of a polar vinyl alcohol component for effective gas barrier performance[1] and are not compatible with nonpolar HDPE. In contrast to the coextrusion process, the laminar-blend blow-molding process forms a layered structure containing numerous discontinuous, overlapping platelets of barrier resins such as PA, poly(vinyl alcohol) (PVA), and ethylene vinyl alcohol (EVOH) in a PE matrix. This is one of the well-proven barrier technologies used to enhance the resistance of PE containers to hydrocarbon permeation.[9–12] Because PE/PA, PE/PVA, and PA/EVOH blends are thermodynamically immiscible and mechanically incompatible, compatibilizer precursor (CP) resins have often been used to improve the interfacial properties between PE and PA, PVA, and EVOH and to enhance the barrier properties of PE/PA/CP blends. These heterogeneous laminar blends exhibit significantly higher permeation barrier properties than conventional homogeneous blends associated with PA uniformly dispersed within the PE matrix.[13–15]

Further investigations have determined that these barrier properties of PE/PA/CP blends depend greatly on the manner of blending and on the resulting morphology.[14–16] Our latest studies[17–20] have indicated that the types and contents of CP and PA present in a modified polyamide (MPA) have significant effects on the barrier, morphology, and rheological properties of MPA resins and the corresponding polyethylene/modified polyamide (PE/MPA) blends. In addition, the melt shear viscosities of PE and MPA have a significant influence on the deformation and morphology of MPA during the blow-molding process of PE/MPA blends. Clearly defined laminar structures of MPA are always observed at some particular values of the melt shear viscosity ratios of MPA to PE. Such clearly defined laminar structures often accompany the highest permeation resistance to xylene. These particular values of the melt shear viscosity ratios were called the optimum viscosity ratios in our previous study, and the value of the optimum viscosity ratio varies as the composition of MPA changes.[21–23] With the proper compositions and processing conditions,[23,24] the xylene permeation resistance of PE/MPA bottles at 28°C can be made about 250 times better than that of pure PE bottles.

In our latest investigation,[25] we found that these laminar-blend structured bottles have excellent permeation resistance even against mixtures of nonpolar hydrocarbon solvents (e.g., paint thinner). After blending 10 wt % of the proper composition of MPA in PE and carefully controlling the MPA morphology in the PE/MPA bottles, we discovered that the white spirit permeation rates of the PE/MPA bottles at 40°C were about 365 times slower than that of the PE bottles.[25] However, significantly poor permeation resistance was found[13,25,26] for these laminar-blend structured bottles when the PE/MPA bottles were filled with mixtures of polar and nonpolar solvents (i.e., gasoline and paint mixed solvents). With the proper compositions,[13,25] the gasoline permeation resistance of the PE/MPA bottles at 40°C was only about 130 times better than that of pure PE bottles. Even after the proper annealing treatment, the barrier property of the PE/MPA bottles was only 190 times better than that of the pure PE bottles. Moreover, much worse barrier improvement (<15) against the permeation of a paint mixed solvent was found for the PE/MPA bottles when the polar solvents were in a certain range.[25] Our latest study[27] found much better barrier properties and more clearly defined MPA and modified polyamide–ethylene vinyl alcohol copolymer (MPAEVOH) laminas for PE/MPA and polyethylene/modified polyamide–ethylene vinyl alcohol copolymer (PE/MPAEVOH) bottles, respectively. In fact, with the proper composition, the gasoline permeation rate of the PE/MPAEVOH bottles was about 450 and 3 times slower than that of the PE and PE/MPA bottles, respectively.

The main objective of this study was to investigate the oxygen barrier properties of PE, polyethylene/ethylene vinyl alcohol copolymer (PE/EVOH), polyethylene/modified ethylene vinyl alcohol copolymer (PE/MEVOH), and PE/MPAEVOH bottles and to optimize the compositions of PE/MEVOH and PE/MPAEVOH bottles to further enhance their oxygen barrier properties. In fact, with the proper MPAEVOH compositions, the oxygen permeation resistance of the PE/MPAEVOH bottles was even significantly better than that of the PE/EVOH bottles. These interesting oxygen barrier and morphological properties of PE, PE/EVOH PE/MEVOH, and PE/MPAEVOH bottles were investigated in terms of the free volumes, barrier properties, and molecular interactions in the amorphous-phase structure of the barrier resins present in their corresponding bottles.

EXPERIMENTAL

Materials and sample preparation

PA and CP were obtained from Formosa Chemicals and Fiber Corp. (Chughua, Taiwan); PA was nylon 6 with the trade name of Sunylon 6N, and CP was a zinc-neutralized ethylene/acrylic acid copolymer. The MPA resin was prepared by the reactive extrusion of the melt blending of CP and PA. PE (HDPE Taisox 9003), EVOH samples of various viscosities with 32 mol % ethylene, and an antioxidant (Irganox B225) were obtained from Formosa Plastic Corp. (Taipei, Taiwan), Kuraray Corp. (Osaka, Japan), and Ciba–Geigy Corp. (Basel, Switzerland), respectively.

Before the melt blending, PA was dried at 80°C for 16 h in air, whereas EVOH and CP were dried at 60°C for 16 h. About 1500 ppm of the antioxidant was dry-blended with the dried blends of PA/CP and EVOH/CP at various weight ratios. The dry-blended PA/CP and EVOH/CP with the antioxidant were then fed into an Ekegai PCM 45 corotating twin-screw extruder (Taoyuan, Taiwan) to make the MPA and modified ethylene vinyl alcohol copolymer (MEVOH) resins, respectively. The extruder was operated at 220°C in the feeding zone and at 240°C toward the extrusion die with a screw speed of 100 rpm. The MPA and MEVOH obtained from the twin-screw extruder were quenched in cold water at 15°C and cut into pellets. The blends of MPA and EVOH (MPAEVOH) were prepared through the melt blending of MPA and EVOH with a Fure Shuen 40SP-H single-screw extruder. The dried components of MPA/EVOH at various weight ratios were fed into the single-screw extruder (Wugwo, Taiwan) operating at 220°C in the feeding zone and at 235°C toward the extrusion die with a screw speed of 400 rpm. The extruded MPAE-

TABLE I
Compositions of the MEVOH and MPAEVOH Resins

Sample	PA (%)	EVOH (%)	CP (%)
MEVOH$_{10}$	—	90.00	10.00
MEVOH$_{20}$	—	80.00	20.00
MEVOH$_{40}$	—	60.00	40.00
MPA$_1$EVOH$_4$	17.00	80.00	3.00
MPA$_1$EVOH$_3$	21.25	75.00	3.75
MPA$_1$EVOH$_2$	28.33	66.67	5.00
MPA$_1$EVOH$_1$	42.50	50.00	7.50
MPA$_2$EVOH$_1$	56.67	33.33	10.00
MPA$_4$EVOH$_1$	68.00	20.00	12.00

VOH resins were then quenched in cold water at 15°C and cut into pellets. The compositions of the MEVOH and MPAEVOH specimens are summarized in Table I.

Before the film blowing, MPA and MPAEVOH resins were dried at 80°C for 16 h, whereas EVOH and MEVOH resins were dried at 60°C for 16 h. These barrier resins were coextruded with the HDPE resin and then film-blown with a Lung-Jeng LM/AH40MI double-layer blown-film machine (Tainan, Taiwan) because it is well known that the melt viscosities of these barrier resins are too low for the films to be blown alone. The extruder used for HDPE was operated at 195°C in the feeding zone and at 200°C toward the extrusion die with a screw speed of 150 rpm and at 195°C in the feeding zone and at 230°C toward the extrusion die with a screw speed of 150 rpm. The coextruded films were then blown up at a blow-up ratio of 3; the HDPE and barrier resins were in the inside and outside layers, respectively. After the film blowing, the barrier layers were separated from the HDPE layer. The barrier film specimens prepared in this study were 25 μm thick.

Before the blow molding, dried MPA, EVOH, MEVOH, and MPAEVOH resins were dry-blended with HDPE at a 10 : 90 weight ratio. The PE/MPA, PE/EVOH, PE/MEVOH, and PE/MPAEVOH blends were then blow-molded in a TPH-550 extrusion blow-molding machine with an extrusion temperature of 230°C and a screw speed of 400 rpm. The extrusion blow-molding machine was purchased from Jonh-Huah Corp. (Tainan, Taiwan). A conventional PE screw was used to extrude the PE/MPA, PE/MEVOH, and PE/MPAEVOH blends before blow molding. The blow-molded bottles weighed about 100 g and had a capacity of about 750 mL and a wall thickness of about 2 mm. For comparison, bottles were also prepared from pure PE resin with the same screw and blow-molding machine, but it was operated at an extrusion temperature of 190°C and at a screw speed of 400 rpm.

Oxygen permeation tests of MPA, EVOH, MEVOH, and MPAEVOH films and PE, PE/MPA, PE/EVOH, PE/MEVOH, and PE/MPAEVOH bottles

The oxygen permeation rates of PE, PA, MPA, MEVOH, and MPAEVOH films were determined with a Lyssy L100-4002 manometric gas permeability tester (Kyoto, Japan) in agreement with the ASTM D 1434 standard. All the film specimens were cut into circles 10 cm in diameter and about 25 μm thick. All the permeation tests were carried out at 25°C and 65% relative humidity. The oxygen permeation rate of each film specimen was estimated on the basis of the average permeation rate of at least three film specimens.

The bottle specimens were purged with nitrogen 99.999% pure and then were sealed with a sleeve stopper before any permeation testing. The sleeve-stopper-sealed bottles were then placed in an oven operated at 35°C and 40% relative humidity. The concentrations in the bottles were determined every 24 h for 14 days with a China 8900 gas chromatography instrument (Taipei, Taiwan) equipped with a thermal conductivity detector. The oxygen concentration of each bottle was estimated on the basis of the average oxygen concentration of at least three bottle specimens. The oxygen permeation rates of PE, PE/MPA, PE/EVOH, PE/MEVOH, and PE/MPAEVOH bottles were evaluated according to the oxygen concentration increase in the bottles after the permeation tests.

Free-volume properties

The free-volume characteristics of the polymers were determined with a positron annihilation lifetime instrument equipped with a fast–fast coincidence spectrometer and a ^{22}Na source that was sandwiched between a number of films on both sides to ensure complete annihilation of the positrons in the sample. A short-lived component (τ_1; ca. 0.12 ns), an intermediate-lived component (τ_2; ca. 0.35–0.4 ns), and a long-lived component (τ_3; ca. 1.8–2.5 ns) were the three resolved lifetime components obtained, and they were attributed to the *para*-positronium, free positron, and *ortho*-positronium (*o*-Ps) states, respectively. The annihilation of *o*-Ps in the spherical free-volume cavities can be described by a simple quantum mechanical model, which assumes the *o*-Ps atom to be localized in a spherical potential well with an electron layer of thickness ΔR. This model provides the relationship between the radius of the free-volume cavities (R_f) and the *o*-Ps lifetime (τ_3) as follows:[28]

$$\frac{1}{\tau_3} = 2\left[1 - \frac{R_f}{R_0} + \frac{1}{2\pi}\sin\left(\frac{2\pi R_f}{R_0}\right)\right] \qquad (1)$$

where R_0 is equal to $R_f + \Delta R$. ΔR was determined by the fitting of the experimental values of τ_3 obtained for materials of known hole sizes, such as zeolites. The ΔR value of 1.66 Å was used in this study.[28]

Thermal and rheological properties

The thermal properties of PE, PA, CP, EVOH, MEVOH, MPA, and MPAEVOH resins were deter-

TABLE II
Thermal Properties of the PE, CP, MPA, EVOH, MEVOH, and MPAEVOH Resins

Parameter	Sample						
	PE	CP	MPA	EVOH	$MEVOH_{10}$	$MEVOH_{20}$	$MEVOH_{40}$
T_M (°C)	131.2	92.4	220.7	183.4	182.0	180.9	179.4
W_C (%)	69.7	25.9	27.5	75.8	60.9	51.6	44.8

Parameter	Sample											
	MPA_1EVOH_4		MPA_1EVOH_3		MPA_1EVOH_2		MPA_1EVOH_1		MPA_2EVOH_1		MPA_4EVOH_1	
	EVOH	MPA	EVOH	MPA	EVOH	MPA	EVOH	MPA	EVOH	MPA	EVOH	MPA
T_M (°C)	182.7	215.0	182.6	215.1	181.4	215.6	180.3	215.6	—	219.2	—	219.8
W_C (%)	58.8		53.5		43.5		33.7		30.7		33.3	

mined with a DuPont 2010 differential scanning calorimetry (DSC) instrument (New Castle, DE). All scans were carried out at a heating rate of 10°C/min and under flowing nitrogen at a flow rate of 25 mL/min. The instrument was calibrated with pure indium. Samples weighing about 15 or 0.5 mg were placed in standard aluminum sample pans for crystallinity percentage (W_c) and melting temperature (T_m) measurements. The W_c values of PE and CP were estimated with baselines drawn from 30 to 160°C and with a perfect heat of fusion of 293 J/g,[29] whereas a perfect heat of fusion of 190 J/g[30] and baselines drawn from 185 to 250°C were used for evaluating the W_c values of PA and MPA present in MPAEVOH. The W_c values of EVOH and MEVOH present in MPAEVOH were evaluated with baselines drawn from 150 to 185°C and a perfect heat of fusion of 107 J/g.[31] The baselines used in the experiments were adjusted to have a maximum fluctuation of less than 0.04 mW over the temperature range of interest. With these baselines, the maximum variation of the heat of fusion was normally around 3 J/g, which resulted in a 1% error in estimating the W_c value.

The melt shear viscosities of PE, CP, MPA, EVOH, MEVOH, and MPAEVOH resins were measured at 230°C and at shear rates ranging from 15 to 120 1/s with a Rosand precision advanced capillary extrusion rheometer (West Midlands, UK) equipped with a capillary 1 mm in diameter. Before the testing, CP, EVOH, and MEVOH were dried at 60°C for 8 h, whereas PA, MPA, and MPAEVOH were dried at 80°C for 16 h. These melt shear viscosities, measured at various shear rates up to about 100 1/s, were used to correlate the deformation behavior of EVOH, MPA, MEVOH, and MPAEVOH in PE during the blow molding of PE/EVOH, PE/MPA, PE/MEVOH, and PE/MPAEVOH blends, respectively, because the shear rates of the polymer melts during extrusion and blow molding are generally recognized to be less than 100 1/s.

Morphology of PE/EVOH, PE/MPA, PE/MEVOH, and PE/MPAEVOH bottles

To observe the deformation structures of EVOH, MPA, MEVOH, and MPAEVOH resins in PE/EVOH, PE/MPA, PE/MEVOH and PE/MPAEVOH bottles, respectively, we first sectioned these bottles with a scalpel, and then we etched them with formic acid. The etched samples were gold-coated and examined with a JEOL JSM-5200 scanning electron microscope (Tokyo, Japan).

RESULTS AND DISCUSSION

Thermal and rheological properties of CP, MPA, EVOH, MEVOH, and MPAEVOH resins

W_c and T_m for CP, MPA, EVOH, MEVOH, and MPAEVOH resins are summarized in Table II. EVOH exhibits lower T_m but much higher W_c values than MPA, whereas CP shows the lowest W_c and T_m values if the three base resins. W_c and T_m of MEVOH resins are significantly lower than those of the base EVOH resin and decrease consistently as the CP contents present in the MEVOH resins increase. As indicated in our recent investigation,[32] the formation of CP-grafted EVOH copolymers through the reaction of carboxylic acid groups of CP with the hydroxyl groups of EVOH can be found during the preparation of MEVOH resins. Presumably, this decrease in W_c and T_m is attributable to the possibly formed CP-grafted EVOH copolymer during the reactive extrusion of MEVOH resins because the presence of the CP-grafted EVOH copolymer in MEVOH resins can interfere with and inhibit the crystallization of EVOH molecules during the crystallization process and, therefore, significantly reduce T_m and W_c of MEVOH resins as their CP contents increase.

As shown in Table II, the W_c values of MPAEVOH resins are lower than those of the base EVOH, and they decrease consistently with increasing MPA contents in MPAEVOH resins. Typical DSC thermograms
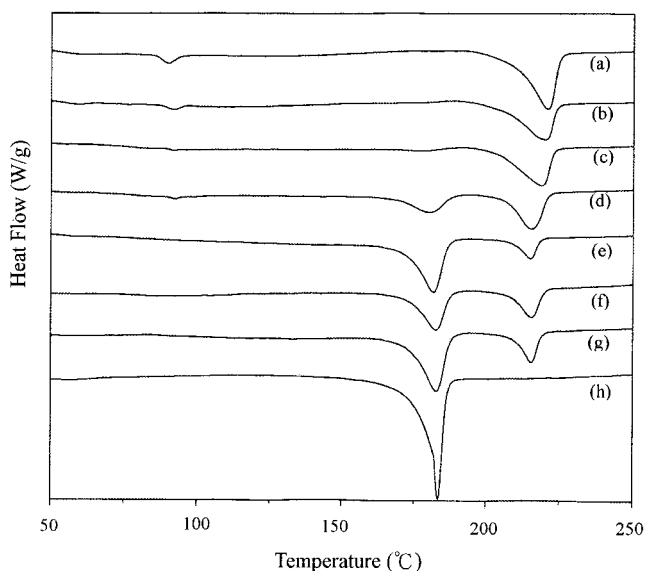
Figure 1 DSC thermograms of (a) MPA, (b) MPA$_4$EVOH$_1$, (c) MPA$_2$EVOH$_1$, (d) MPA$_1$EVOH$_1$, (e) MPA$_1$EVOH$_2$, (f) MPA$_1$EVOH$_3$, (g) MPA$_1$EVOH$_4$, and (h) EVOH specimens.

Figure 2 Melt shear viscosities of (—) CP, (○) PE, (◇) PA, (□) MPA, and (▲) EVOH resins measured at various shear rates.

of MPA, EVOH, and MPAEVOH resins are shown in Figure 1. The main melting endotherms with peak temperatures of approximately 183 and 225°C can be found in the DSC thermograms of EVOH and MPA resins, respectively. As shown in the DSC thermogram of the MPA resin, the small melting endotherm with a peak temperature of about 90°C is most likely due to the melting of the residual traces of CP present in MPA. After the blending of EVOH in MPA, the peak temperatures associated with the main melting endotherm of MPA and EVOH decrease significantly with increasing EVOH and MPA contents in the MPAE-VOH resins, respectively. However, the melting endotherm associated with the EVOH resin disappears quickly as the MPA contents present in MPAEVOH increase. In fact, almost no EVOH melting endotherm can be found in the MPAEVOH thermograms when the MPA contents reach about 66.7 and 80 wt % (i.e., MPA$_2$EVOH$_1$ and MPA$_4$EVOH$_1$).

The melt shear viscosities of CP, PE, PA, MPA, EVOH, MEVOH, and MPAEVOH resins measured at various shear rates are summarized in Figures 2–4. The melt shear viscosities of all the resins decrease as the shear rate increases. Among these resins, PE and EVOH exhibit the highest and lowest melt shear viscosities, respectively (see Fig. 2). The melt shear viscosities of MPA measured at various shear rates are very close to those of PE and significantly higher than those of PA without CP modification. As indicated in our previous investigations,[17–20] this increase in the melt shear viscosity of MPA is attributable to the formation of CP-grafted PA copolymers during the preparation of the MPA resin because the reaction between the carboxylic acid groups of CP with the
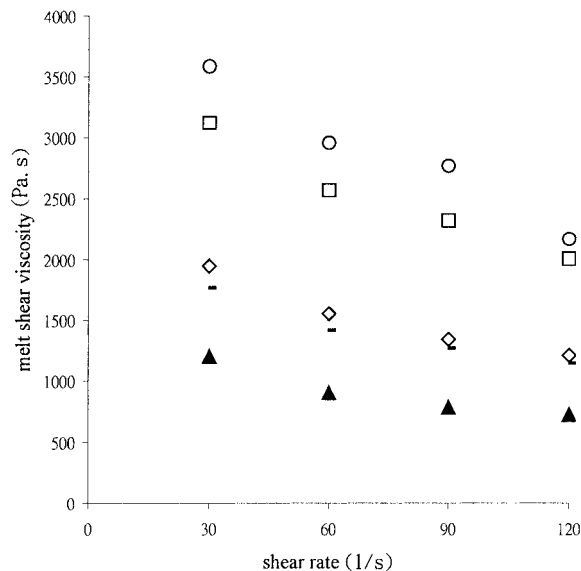
terminal amine groups of PA is found during the reactive extrusion of CP and PA resins. Similar to those of the MPA resin, the melt shear viscosities of MEVOH resins increase significantly as the CP contents present in MEVOH increase (see Fig. 3). Presumably, this increase in the melt shear viscosity of MEVOH is attributable to the possibly formed CP-grafted EVOH copolymers during the reactive extrusion of MEVOH resins because the crosslinked struc-
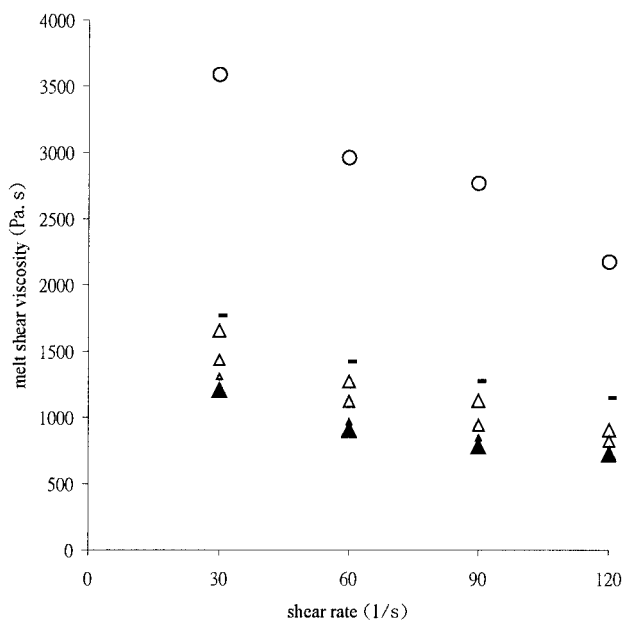

Figure 3 Melt shear viscosities of (—) CP, (○) PE, (▲) EVOH, (△) MEVOH$_{10}$, (△) MEVOH$_{20}$, and (△) MEVOH$_{40}$ resins measured at various shear rates.
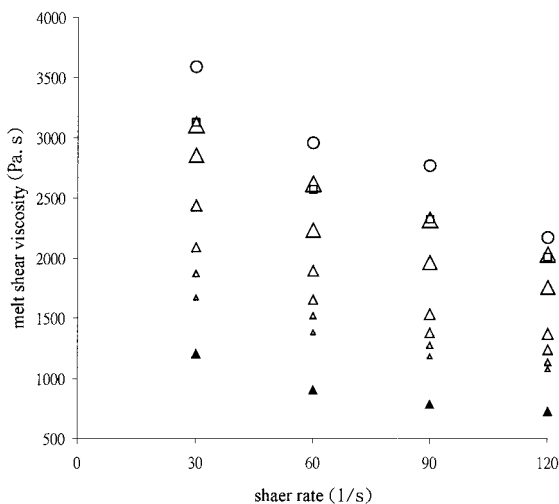
Figure 4 Melt shear viscosities of (○) PE, (□) MPA, (▲) EVOH, (△) MPA$_4$EVOH$_1$, (△) MPA$_2$EVOH$_1$, (△) MPA$_1$EVOH$_1$, (△) MPA$_1$EVOH$_2$, (△) MPA$_1$EVOH$_3$, and (△) MPA$_1$EVOH$_4$ measured at various shear rates.

tures of CP-grafted EVOH copolymers can cause the melt shear viscosities of MEVOH to increase. After the blending of MPA in EVOH, the melt shear viscosities of MPAEVOH resins measured at various shear rates are higher than those of the EVOH resin and increase consistently with increasing MPA contents in the MPAEVOH resins (see Fig. 4). Somewhat surprisingly, the melt shear viscosities of some MPAEVOH samples are even higher than those of the base MPA resin measured at various shear rates as their MPA contents reach about 80 wt % (e.g., MPA$_4$EVOH$_1$).

Free-volume properties

Table III summarizes the free-volume properties of PE, CP, PA, MPA, and EVOH resins. As expected, PE and EVOH exhibit the largest and smallest average volumes of the free-volume cavities (V_f) and R_f values, respectively, among these base resins. In comparison with PA, MPA exhibits a slightly larger R_f value, which is still significantly smaller than those of PE and CP specimens. The R_f values of MEVOH specimens are significantly larger than those of their correspond-

TABLE III
Free-Volume Properties of the PE, CP, PA, MPA, and EVOH Resins

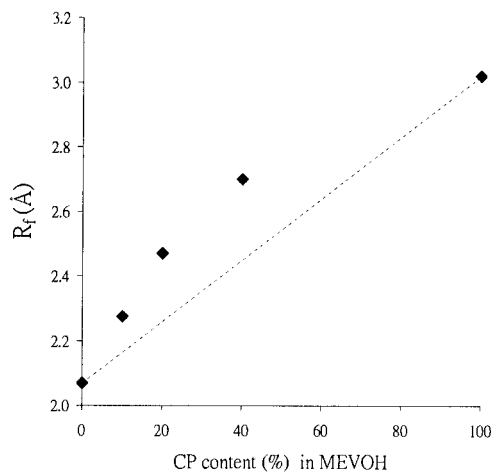| Sample	R_f (Å)	V_f (Å^3)
PE	3.04	117.73
CP	3.02	115.26
PA	2.32	52.52
MPA	2.45	61.92
EVOH	2.07	37.09

Figure 5 R_f for the MEVOH sample series.

ing base EVOH resins, and they increase consistently as the CP contents in MEVOH increase (see Fig. 5). For instance, the R_f values of MEVOH specimens increase from 2.07 to 2.7 Å as the CP contents in MEVOH increase from 0 to 40 wt %. Presumably, this increase in R_f is attributable to the possibly formed CP-grafted EVOH copolymer during the reactive extrusion of MEVOH resins because the formation of the CP-grafted EVOH copolymer in MEVOH resins can break not only the hydrogen bonds but also the dense molecular structure present in the amorphous phases of EVOH resins. As a result, the R_f values of MEVOH resins decrease significantly as their CP contents increase.

Figure 6 summarizes the free-volume properties of MPAEVOH resins. The R_f values of the MPAEVOH sample series increase consistently as the MPA contents in MPAEVOH increase. It is not completely clear what accounts for the interesting thermal, rheological, and free-volume properties described in the previous two sections. However, as indicated in our latest in-
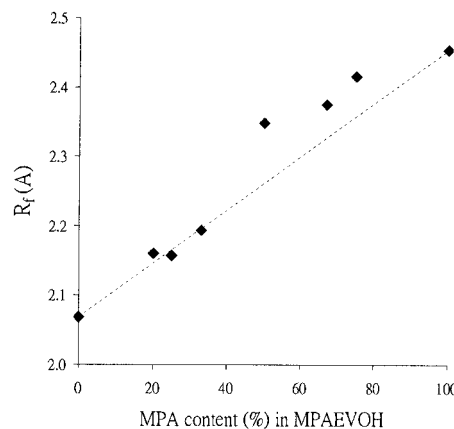

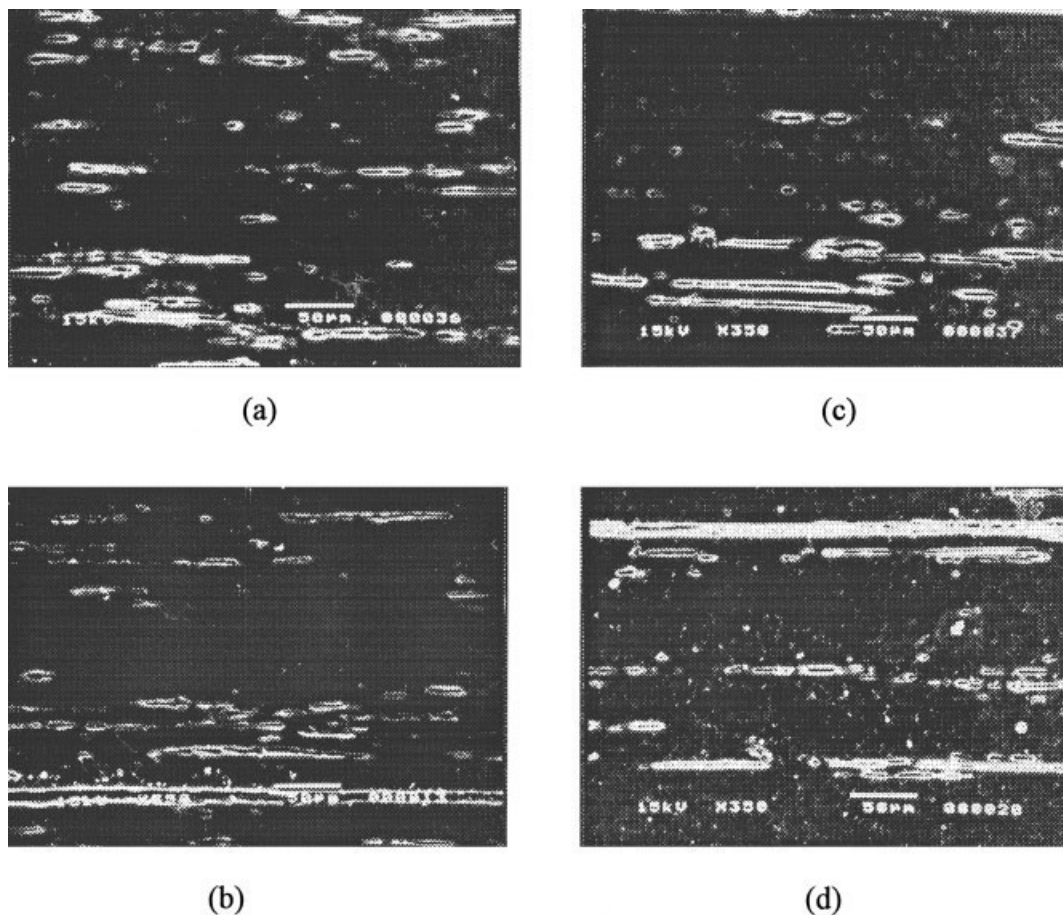**Figure 6** R_f for the MPAEVOH sample series.

Figure 7 Fracture surfaces of (a) PE/EVOH, (b) PE/MEVOH$_{10}$, (c) PE/MEVOH$_{20}$, and (d) PE/MEVOH$_{40}$ bottle specimens.

vestigation,[32] the presence of MPA can interfere with or break the hydrogen bonds originally present in EVOH resins because new hydrogen bonds are found through the interaction of the carbonyl and amide groups of MPA with the hydroxyl groups of EVOH resins. In fact, the X-ray diffraction peak corresponding to EVOH crystals and self-associated hydroxyl–hydroxyl bonds within EVOH resins disappear when the EVOH concentrations in MPAEVOH specimens are less than 20 wt %.[32] On the basis of these premises, it is reasonable to suggest that MPA and EVOH in MPAEVOH resins can interfere with each other and possibly cocrystallize; therefore, the melting peak temperatures of both EVOH and MPA can be reduced significantly with increasing MPA and EVOH contents, respectively. However, after the blending of MPA in the EVOH resin, the dense molecular structure originally present in the amorphous regions of EVOH specimens is disrupted and changed into a sparser structure as the MPA contents increase. As a result, the R_f values of the MPAEVOH specimens are larger than that of the base EVOH resin and increase significantly as the MPA contents increase. However, making EVOH molecules soluble in the MPA-rich phase without phase separation is easier than making

MPA molecules soluble in the EVOH-rich phase without phase separation. In fact, at some optimum MPAEVOH compositions, EVOH can be blended in MPA-rich phases without or with only slight phase separation; the EVOH molecules are miscible and strongly interact with the MPA molecules. Under such circumstances, the melt shear viscosities of the MPA$_4$EVOH$_1$ resin are even higher than those of the base MPA resin measured at various shear rates.

Morphology of PE/EVOH, PE/MEVOH, PE/MPA, and PE/MPAEVOH bottles

Typical micrographs of the fracture surfaces of PE/EVOH, PE/MEVOH, PE/MPA, and PE/MPAEVOH bottles are summarized in Figures 7 and 8. As shown in Figure 7, only dispersed EVOH droplets or agglomerates were found on the fracture surfaces of PE/EVOH bottles, but somewhat obscurely defined EVOH laminas were found distributed in PE matrices through the wall thickness direction of PE/MEVOH bottles. In contrast, more clearly defined laminas were found on the fracture surfaces of PE/MPAEVOH bottles as the MPA contents present in MPAEVOH increased (see Fig. 8). These results suggest that PE can
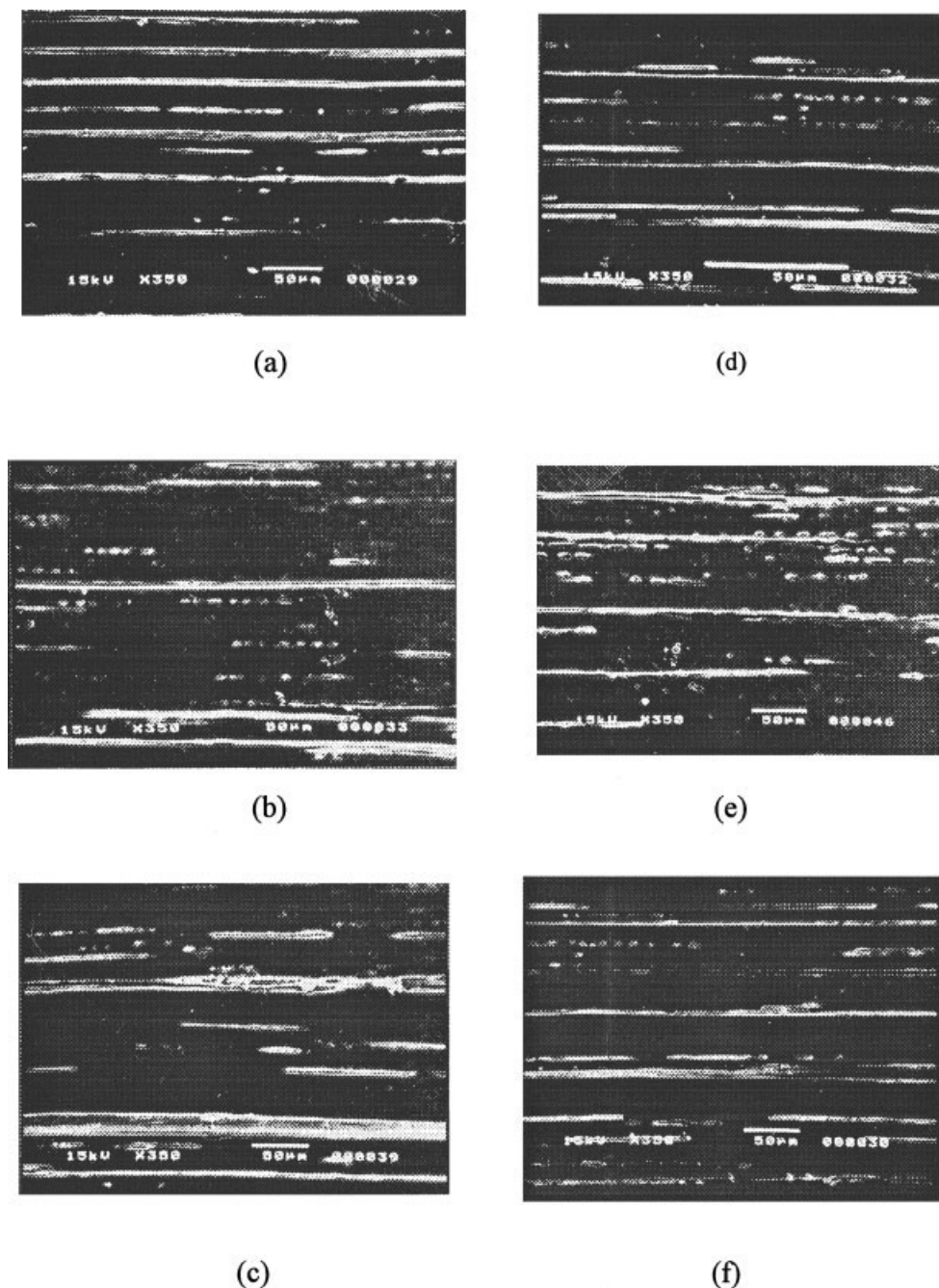
Figure 8 Fracture surfaces of (a) PE/MPA, (b) PE/MPA$_1$EVOH$_3$, (c) PE/MPA$_1$EVOH$_2$, (d) PE/MPA$_1$EVOH$_1$, (e) PE/MPA$_2$EVOH$_1$, and (f) PE/MPA$_4$EVOH$_1$ bottle specimens.

easily stretch MPA into elongated laminas because MPA is modified to adhere well to the PE matrix and is not too hard or too soft to draw into continuous laminar structures during the blow-molding process of PE/MPA blends. In contrast, the interfacial adhesion between PE and EVOH is not good enough to keep PE from stretching EVOH into elongated and demarcated laminas during the blow-molding process of PE/EVOH blends. Presumably, the MEVOH melts are not strong enough to draw into continuous lami-

nar structures, although the interfacial adhesion between PE and MEVOH is improved after EVOH is modified with CP. After the blending of MPA in the EVOH resin, the MPA-rich phases continue to grow at the expense of the EVOH-rich phases; the MPA-rich phases are believed to adhere well to the PE matrix and can be drawn by the PE matrix into continuous laminar structures better than the EVOH-rich phases. Under such circumstances, more elongated and demarcated MPAEVOH laminas were found on the frac-

TABLE IV
Oxygen Permeation Rates of the PE, PE/PA, PE/MPA,
PE/EVOH, and PE/MEVOH Bottle Specimens at 35°C

	Oxygen permeation rate (%/day)	Oxygen barrier improvement
Blow-molded specimen		
PE	0.756	1
PE/PA	0.329	2.30
PE/MPA	0.318	2.38
PE/EVOH	0.225	3.36
PE/MEVOH sample series		
PE/MEVOH$_{10}$	0.242	3.12
PE/MEVOH$_{20}$	0.262	2.88
PE/MEVOH$_{40}$	0.316	2.39

ture surfaces of PE/MPAEVOH bottles when the MPA contents in MPAEVOH increased. These clearly defined laminar structures of the barrier resins can further prolong the permeation time of oxygen molecules and, therefore, enhance the barrier properties of their corresponding bottles.

Oxygen permeation properties of PE, PE/EVOH, PE/MEVOH, PE/MPA, and PE/MPAEVOH bottles

The oxygen permeation rates of PE, PE/EVOH, PE/MEVOH, PE/MPA, and PE/MPAEVOH bottles at 35°C are summarized in Table IV. The PE bottles show the worst oxygen barrier properties of these bottles; about 0.756 mol % oxygen permeates into the nitrogen-filled PE bottles per day at 35°C. After the blending of 10 wt % barrier resins in PE, the oxygen barrier properties of PE/PA, PE/MPA, and PE/EVOH bottles improve significantly with respect to those of plain PE bottles. As expected, PE/EVOH bottle specimens exhibit significantly slower oxygen permeation rates than PE/PA and PE/MPA bottle specimens. Somewhat surprisingly, the oxygen permeation rates of each PE/MEVOH bottle series are significantly faster than those of their corresponding PE/EVOH bottle specimens. Moreover, the oxygen permeation rates of each PE/MEVOH bottle series increase consistently with the CP contents in the MEVOH resins. However, after the blending of MPA in EVOH, the oxygen permeation rates of each PE/MPAEVOH bottle series are dramatically slower than those of the PE/EVOH bottle (see Table V). This improvement in the oxygen barrier properties of PE/MPAEVOH bottles continues as the EVOH contents present in MPAEVOH reach the optimum content. In fact, at a 1 : 3 weight ratio of MPA to EVOH, the value of the oxygen barrier improvement of each PE/MPAEVOH bottle series reaches the maximum; the oxygen permeation rates of PE/MPA$_1$EVOH$_3$ bottle specimens are even slower than those of the corresponding PE/EVOH bottles and are about 4.5–5.0 times slower than those of PE bottles. It

is not completely clear what accounts for these interesting oxygen barrier properties. It is generally recognized that gas or liquid permeant molecules can hardly diffuse through crystalline regions but can only permeate through the amorphous regions of the polymer resins; the permeant paths in the amorphous regions offer enough space to allow permeant molecules to enter and diffuse. It is, therefore, reasonable to suggest that the sizes of the free-volume cavities and the compositions in the amorphous regions of the polymers can greatly affect their barrier properties. On the basis of these premises, it is not hard to believe that small nonpolar oxygen molecules with an effective radius of about 2 Å can easily enter and permeate the nonpolar amorphous regions of PE resins with a relatively large R_f value of about 3 Å. In contrast, the smallest R_f value (ca. 2.05 Å) and polar hydroxyl groups in the amorphous regions of EVOH resins can significantly inhibit the nonpolar oxygen molecules, in comparison with PE, PA, MPA, and MEVOH resins, from entering and permeating their amorphous regions. As a result, PE/EVOH bottle specimens exhibit better oxygen permeation resistance than PE, PE/PA, and PE/MPA bottle specimens, although their laminar structures are not as clearly defined as those of PE/MPA and PE/MEVOH bottle specimens.

However, as mentioned in the previous section, broken and less demarcated MPAEVOH laminas were found on the fracture surfaces of PE/MPAEVOH bottles as the EVOH contents increased. Presumably, these broken and less demarcated laminas can cause deleterious effects on the oxygen barrier properties of PE/MPAEVOH bottles and counterbalance the beneficial effects caused by the presence of EVOH in MPAEVOH resins because EVOH molecules have smaller R_f values than MPA molecules and can enhance the barrier properties of MPAEVOH resins as the EVOH contents increase. It is, therefore, reasonable to understand that an optimum PE/MPAEVOH bottle specimen (i.e., PE/MPA$_1$EVOH$_3$) exhibits better oxygen permeation resistance than PE/EVOH and

TABLE V
Oxygen Permeation Rates of the PE, PE/PA, PE/MPA,
and PE/MPAEVOH Bottle Specimens at 35°C

Blow-molded specimen	Oxygen permeation rate (%/day)	Oxygen barrier improvement
PE	0.756	1
PE/PA	0.329	2.30
PE/MPA	0.318	2.38
PE/MPA$_4$EVOH$_1$	0.319	2.37
PE/MPA$_2$EVOH$_1$	0.215	3.51
PE/MPA$_1$EVOH$_1$	0.205	3.7
PE/MPA$_1$EVOH$_2$	0.201	3.76
PE/MPA$_1$EVOH$_3$	0.150	5.05
PE/MPA$_1$EVOH$_4$	0.175	4.32

other PE/MPAEVOH bottles; the MPAEVOH resins are associated with relatively elongated and demarcated laminar structures and small R_f values.

CONCLUSIONS

PE bottles exhibited the worst oxygen barrier properties of the bottles; about 0.756 mol % oxygen permeated into nitrogen-filled PE bottles per day at 35°C. After the blending of 10 wt % barrier resins in PE, the oxygen barrier properties of PE/PA, PE/MPA, and PE/EVOH bottles were significantly better than those of plain PE bottles. However, after the blending of MEVOH barrier resins in PE matrices, the oxygen permeation rates of each PE/MEVOH bottle series were significantly faster than those of their corresponding PE/EVOH bottle specimens. In addition, the oxygen permeation rates of each PE/MEVOH bottle series increased consistently with the CP contents in the MEVOH resins. After the blending of proper compositions of MPA in EVOH, the more elongated and demarcated MPAEVOH laminas with relatively small R_f values further enhanced the oxygen permeation resistance of PE/MPAEVOH bottle specimens, making it better than that of PE/EVOH bottle specimens. In fact, at a 1 : 3 weight ratio of MPA to EVOH, the value of the oxygen barrier improvement of the PE/MPAEVOH bottle series reached the maximum; the oxygen permeation rates of the PE/MPA$_1$EVOH$_3$ bottle specimen were even slower than those of the corresponding PE/EVOH bottles and were about 4.5–5.0 times slower than those of the PE bottles. These interesting oxygen barrier and morphological properties of PE, PE/EVOH PE/MEVOH, and PE/MPAEVOH bottles were investigated in terms of the free volumes, barrier properties, and molecular interactions in the amorphous-phase structures of the barrier resins present in their corresponding bottles.

References

1. Iwanamy, T.; Hiral, Y. Tappi J 1983, 66, 85.
2. Tanaka, Y. Jpn Food Sci 1989, 7, 49.
3. Ozeki, Y.; Kim, J. Polymeric Materials Encyclopedia; CRC: New York, 1996; Vol. 3.
4. Finch, C. A. Polyvinyl Alcohol; Wiley: New York, 1992.
5. Koros, W. J. Barrier Polymers and Structures; ACS Symposium Series 423; American Chemical Society: Washington, DC, 1989.
6. Finlayson, K. M. Plastic Film Technology: High Barrier Plastic Film for Packaging; Technomic: Lancaster, PA, 1989.
7. Odorzynski, T. W. U.S. Pat. 4,347,332 (1982).
8. Pottsville, A. D. U.S. Pat. 4,427,825 (1984).
9. Subramanian, P. M. U.S. Pat. 4,410,482 (1983).
10. Subramanian, P. M. U.S. Pat. 4,444,817 (1984).
11. Yeh, J. T.; Jou, W. S.; Su, Y. S. J Appl Polym Sci 1999, 9, 2158.
12. Yeh, J. T.; Wang, L. H.; Chen, K. N.; Jou, W. S. J Mater Sci 2001, 36, 1891.
13. Yeh, J. T.; Shyu, W. D.; Chen, C. H. J Appl Polym Sci 2001, 80, 1122.
14. Subramanian, P. M. Polym Eng Sci 1985, 25, 483.
15. Subramanian, P. M. Polym Eng Sci 1987, 27, 663.
16. Diluccio, R. C. U.S. Pat. 4,416,942 (1983).
17. Yeh, J. T.; Fan-Chiang, C. C.; Cho, M. F. Polym Bull 1995, 35, 371.
18. Yeh, J. T.; Fan-Chiang, C. C.; Yang, S. S. J Appl Polym Sci 1997, 64, 1531.
19. Yeh, J. T.; Fan-Chiang, C. C. J Appl Polym Sci 1997, 66, 2517.
20. Yeh, J. T.; Fan-Chiang, C. C. J Polym Res 1996, 3, 211.
21. Yeh, J. T.; Jyan, C. F. Polym Eng Sci 1998, 38, 1482.
22. Yeh, J. T.; Jyan, C. F.; Chou, S. Soc Plast Eng Annu Tech Conf 1998, 3, 3567.
23. Yeh, J. T.; Yang, S. S.; Jyan, C. F.; Chou, S. Polym Eng Sci 1999, 39, 1952.
24. Yeh, J. T.; Chao, C. C.; Chen, C. H. J Appl Polym Sci 2000, 76, 1997.
25. Yeh, J. T.; Shih, W. S.; Huang, S. S. Macromol Mater Eng 2002, 287, 23.
26. Yeh, J. T.; Chang, S. S.; Yao, H. T.; Chen, K. N.; Jou, W. S. J Mater Sci 2000, 35, 1.
27. Yeh, J. T.; Huang, S. S.; Yao, W. H. Macromol Mater Eng 2002, 287, 532.
28. Nakanishi, H.; Wang, S. J.; Jean, Y. C. In Positron Annihilation in Fluids; Sharma, S. C., Ed.; World Scientific: Singapore, 1988; p 753.
29. Wunderlich, B. Macromolecular Physics; Academic: New York, 1973; Vol. 1, p 388.
30. Brandrup, J. Polymer Handbook; Wiley: New York, 1989; Chapter 5, p 112.
31. Tubbs, R. K. J Polym Sci Part A: Gen Pap 1965, 3, 4181.
32. Yeh, J. T.; Yao, H. T.; Yao, W. H.; Du, Q. G.; Chen, C. C. J Membrane Sci, submitted.